THEORETICAL AND EXPERIMENTAL STUDIES OF COHERENCE PROPERTIES OF THE COPPER VAPOR LASER RADIATION

V.V. Kolosov and V.O. Troitskii

Institute of Atmospheric Optics,
Siberian Branch of the Russian Academy of Sciences, Tomsk
Received October 20, 1997

The spatial-energetic structure of the radiation of lasers with high gains of active media and short pulse lengths has been investigated. An experimental and theoretical technique is suggested which demonstrates that the radiation of lasers of this type is a superposition of several components and enables the number of these components to be determined along with their divergence and power. The capabilities of this technique are illustrated in the example of determination of the output characteristics of a copper vapor laser.

INTRODUCTION

For a diversity of engineering and pure scientific problems connected with the use of laser radiation data on its spatial coherence (which determines the beam divergence in the far field zone) are of fundamental importance. However, knowledge of the coherence properties alone cannot give a comprehensive idea of the laser radiation pattern. As a rule, in practice the laser radiation comprises highly diverging background component in addition to the main (coherent) one. Therefore, to describe the laser radiation in more detail, at least the data on the amount of background radiation should be added to its characteristics. The problem becomes even more complicated when we consider the radiation comprising several components. In this case, the motion of divergence itself becomes uninformative and it is better to speak about the spatial-energetic beam structure, which is taken to mean the information about the number of these components as well as about the power and divergence of each component.

This spatially inhomogeneous radiation structure is typical of lasers that have:

a) pulsed or pulsed-periodic regime of operation;

b) sufficiently high gains of active media;

c) sufficiently short pulse lengths during which the radiation goes round a resonator no more than $N = 10$ times.

It also should be noted that the component structure is most clearly manifested for unstable resonators in which the coherent beam formation is directly connected with the number of round-trips for radiation in the cavity. Lasers of the above-described type are the subjects of the present study aimed at the development of experimental and theoretical technique that gives information about the spatial and energetic structure of the examined laser.

A study of the coherence properties of the laser radiation is commonly reduced to an analysis of the beam intensity distribution across the focal plane of a lens and in this sense the technique proposed by us is no exception. The problem is how to extract from the known intensity distribution the information about $3N$ unknown parameters (the divergence, the power, and the wavefront curvature of each from N components) that unambiguously determine this intensity distribution.

For $N = 1$ the problem, in essence, is reduced to measurements of the focal spot size

$$\rho_f = \alpha f', \quad f' = R f/(R - f),$$

where α is the divergence of interest to us, f is the focal distance of the lens, and R is the wavefront radius which can be taken infinite in most cases.

For $N = 3$ we tried to solve this problem based on a number of *a priori* assumptions[2] reducing the solution to the adjustment of the values of the most important parameters. However, such an approach to the solution of this problem gives ambiguous results already for $N = 3$ as further investigations have shown, namely, there are many combinations of 3×3 parameters which specify the same intensity distribution within the limits of a measurement error.

To avoid ambiguity, for the proposed technique we first solved the problem about the evolution of the coherence properties of radiation propagating in the system active medium + resonator with the given parameters. As a result, we succeeded in calculating the divergence and the wavefront curvature radius for each radiation component. The unknown weighting energetic coefficients are then adjusted to obtain the best coincidence between the experimental and calculated dependences.

0235-6880/98/02-03 154-05 $02.00

1. EXPERIMENTAL SETUP

Diagram of the experimental setup is shown in Fig. 1.

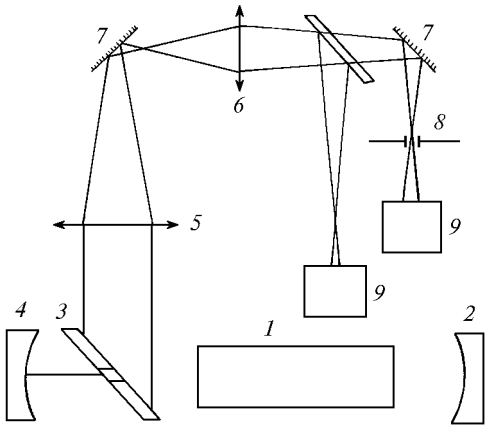

FIG. 1. Diagram of the experimental setup. Here, 1 is the active medium of the copper vapor laser; 2, 3, and 4 are the elements of the unstable confocal resonator: 2 is the spherical mirror (R = 200 cm), 3 is the flat mirror with the aperture (D = 0.08 cm), and 4 is the spherical mirror (R = 10 cm); 5 is the spherical lens (F = 61 cm); 6 is the spherical lens (F = 30.2 cm); 7 is the flat mirror; 8 is the field stop (D = ω); 9 are the power meters.

As an object of investigation we chose a copper vapor laser with an unstable confocal resonator ($M = 20$) which typically generates radiation components (see, for example, Refs. 3 and 4). The laser had a pulse repetition frequency of 7 kHz and a pulse duration of 30 ns (at the pulse base), which provided 8 round-trips for radiation in the cavity. We investigated the stable regime of laser operation. The total average output radiation power was 2 W. The powers of yellow and green lines were in the 2:3 ratio. We measured only the green line.

All optical parts and their location on the propagation path were chosen so that they introduced minimum losses of the background radiation when it propagated from the resonator to the field stop plane. The IMO–2N power meters were used to measure the radiation power. As in Ref. 2, we measured the parameter

$$\eta(\omega) = P_\omega / P_0,$$

rather than the intensity distribution, where P_ω is the power of radiation after passage of the field stop with the diameter ω and P_0 is the power of radiation incident on the field stop.

The behavior of the parameter $\eta(\omega)$ is completely determined by the set of the parameters indicated in the Introduction of the present paper in the same manner as the intensity distribution. We hoped that the minimum number of the optical parts and devices would introduce only small measurement errors. In addition, the ease of measurements and their fully automated character provided the feasibility of measurements in real time.

2. THEORETICAL TECHNIQUE

Calculations of the parameters of propagation of δ-correlated radiation in a medium with nonuniform distribution of the refractive index and gain were done on the basis of the equation for the second-order coherence function

$$\frac{\partial \Gamma_2}{\partial z} + \left[\frac{1}{ik} \nabla_\rho \nabla_{\mathbf{R}} + \frac{k}{2i} \rho \nabla_{\mathbf{R}} \varepsilon(z, \mathbf{R}) + \right.$$

$$\left. + k\, \sigma(z, \mathbf{R})\right] \Gamma_2(z, \mathbf{R}, \rho) = \frac{g_o}{2k^2} W_{\text{eff}}(z, \mathbf{R})\, \delta(\rho), \qquad (1)$$

where $\mathbf{R} = (\rho_1 + \rho_2)/2$ is the summed transverse coordinate, $\rho = \rho_1 - \rho_2$ is the difference transverse coordinate, W_{eff} is the effective intensity of spontaneous emission, ε is the real part of the dielectric constant, σ is the imaginary part of the dielectric constant related with the gain of the medium g by the following expression:

$$\sigma(z, \rho) = - k^{-1} g(z, \rho);$$

and g_o is the gain at the origin of the coordinate system.

This procedure was used to calculate the coherence properties of the output radiation of an X-ray single-pass laser[5,6] representing conceptually an amplifier of spontaneous radiation. Let us now study the propagation of the spontaneous radiation from a given plane X perpendicular to the axis of the active medium (Fig. 2) to the focusing lens F_l.

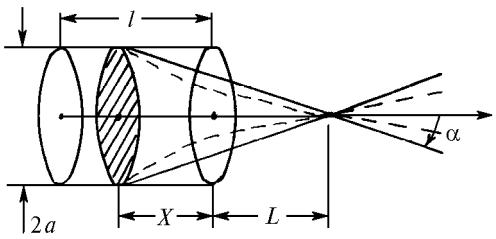

FIG. 2. Scheme of formation of partially coherent radiation coming from point incoherent sources located in a bounded volume.

Given that the refractive index distribution over the cross section of the active medium is uniform and the distribution of spontaneous radiation sources in the plane X which is assumed initial ($z = 0$) is specified in the form

$$W_{\text{eff}}(z, \mathbf{R}) = W_{\delta\,\text{eff}}(\mathbf{R})\, \delta(z),$$

$$W_{\delta\ \text{eff}}(\mathbf{R}) = W_{\delta\,o}(\mathbf{R}) \exp(- R^2/a^2),$$

we obtain for the coherence function in the plane of focusing lens the following expression:

$$\Gamma_2(z = u + L, \mathbf{R}, \rho) = \frac{W_{\delta o}\, g_o}{8\pi(L + X)^2} \times$$

$$\times \exp\left(\int_0^X dz\, g(z)\right) \exp\left(\frac{ik\mathbf{R}\rho}{F}\right) \exp\left(-\frac{\rho^2}{4\rho_c^2}\right), \qquad (2)$$

where $F = X + L$ is the wavefront curvature radius of the partially coherent radiation and

$$\rho_c = (X + L)/(ka) \qquad (3)$$

is its coherence radius equal to the coherence radius defined by the well-known Van Zittert–Zernike theorem.[7]

It follows from solution (2) that the value of the coherence radius is independent of the distribution of the gain g over z. Hence, the beam spot radius in the focal plane of the lens also will be independent of g. However, the radiation coming from different planes inside the active medium will be focused into spots having different radii (for $X = l$ the spot radius will be minimum and for $X = 0$ it will be maximum), because ρ_c and F are functions of X. Therefore, temporal variations of the dependence of g on z may change the relative energy contributions from different planes of the active media and as a consequence, the effective radius of the focal spot produced by radiation coming from all planes also changes.

However, if one of the conditions

$$L \gg F_l \quad \text{or} \quad L \gg l, \qquad (4)$$

is satisfied, the radiation coming from different planes of the active media will be focused into spots of approximately the same radius. Thus, the change of the dependence $g(z)$ changes only the beam intensity in the focal spot but in no way affects its radius.

We have considered above the case of uniform distributions of the refractive index and gain over the cross sections of the active medium. Nonuniform distribution of the refractive index causes the ray bending. Trajectories of rays in case of defocusing are shown by the dashed lines in Fig. 2. Such bending of rays decreases the transverse dimensions of the active medium observed from the plane of the lens and hence increases the coherence radius. In a similar manner, higher values of the gain on the axis of the active medium in comparison with its periphery lead to the decrease of the effective transverse dimensions of the active medium. More comprehensive study of these phenomena based on numerical and analytic solutions of Eq. (1) for an X-ray laser was made in Refs. 5 and 6.

A comparison of the results of our theoretical calculations with the experimental data obtained by us for the copper vapor laser operating in a single-pass (without mirrors) and double-pass (with one mirror) regimes has shown that these effects are insignificant for the copper vapor laser. For this reason, we ignore them further.

3. MAIN RESULTS

Figure 3 shows the equivalent scheme of the experimental setup with the copper vapor laser. Cylinders here represent the active medium repeated infinitely with the help of reflecting mirrors of the resonator represented by equivalent lenses in the figure. Here we did not show some field stops that bounded the laser radiation. They were considered in our calculations together with the field stops shown in Fig. 3. In contrast with Refs. 5 and 6, in our calculations the shape of the coherence function was considered to be Gaussian and remained unchanged when we solved Eq. (1).

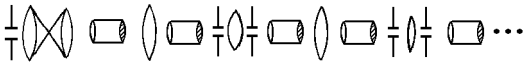

FIG. 3. Equivalent scheme of the experimental setup with the copper vapor laser.

The geometry of the experiment provided that condition (4) was satisfied for all except the first active volumes of the equivalent scheme. This assumption significantly simplified our calculations (without the loss in accuracy), because we calculated the radiation propagation only from the ends of the active volumes rather than from the entire volumes. As a result of these calculations we obtained the output divergence and the output wavefront curvature radius for each volume (radiation component). These parameters are tabulated in Table I. Then we calculated the intensity distributions for each volume in the waist of a telescope. From the results of our calculations it follows that for the laser used in our experiments ($M = 20$) the radiation coming from the fifth and subsequent volumes are focused into spots having diffraction radii.

TABLE I

Serial number of component	Wavefront curvature radius, m			Divergence (diffraction limited)		
	M=20	M=100	M=200	M=20	M=100	M=200
1	0.6	0.6	0.6	320.2	320.2	320.2
2	1.44	144	1.44	107.0	107.0	107.0
3	145	2370	6660	6.0	1.74	1.23
4	340	5440	11100	3.5	1.24	1.07
5	9250	16900	17100	1.04	1.00	1.00
6	11000	16900	17100	1.01	1.00	1.00
8	12500	16900	17100	1.00	1.00	1.00

Thus, the radiation intensity distribution in the waist of the telescope represents a sum of five distributions whose widths are determined by the

geometry of the active medium, resonator, and telescope and are independent of temporal variations of the axial distribution of the gain g within the time over which the pulse acts. However, the energy of each component depends on the variations of g. Whereas the beginning of the pulse the energy of diffraction limited components is small and the total intensity distribution is wide, by the pulse end the most part of energy has already been concentrated in the spot with diffraction limited radius and the total intensity distribution becomes nearly diffraction limited.

The results of calculations for lasers with $M = 100$ and 200 are also tabulated in Table I. It was assumed that the dimensions of the active volume and resonator are identical to those used in our experiment. Only the focal distance of the lens *4* and its separation from the field stop *3* were varied. It can be seen that for $M = 100$ the beam divergence is close to diffraction limited for the fourth component, whereas for $M = 200$ this is true already for the third component.

It is evident that the energy distribution $\eta(\omega)$ measured with the IMO–2N in the waist is averaged over the time during which the pulse acts. Therefore, this technique is capable of determining the weighting energetic coefficients for each radiation component for the period over which the pulse acts. These coefficients are adjusted to provide the best coincidence between the calculated and experimentally measured distributions. The results of this adjustment are illustrated by Fig. 4.

The use of such an approach with the two known parameters (from three) for each component sharply increases the sensitivity of this technique to the deviations of the weighting coefficients from their values at which the best coincidence is achieved between the results of theoretical calculations and experimental measurements (see Fig. 3). It can be seen that changes in the background radiation energy lead to the change in the behavior of the calculated curves on the periphery, in particular, the level of saturation changes. The changes of the energy of the coherent component cause the change of the curve behavior in the axial region. Energy redistribution between the third and the fourth components causes the change of the curve behavior in its central portion. In Ref. 2 these deviations could be compensated through the corresponding changes of the coherence radius and/or the wavefront curvature radius. It has been just this circumstance that leads to ambiguous solution.

From the results shown in Fig. 4 it follows that the background component of radiation carries ~20% of the total energy and the coherent component carries ~30%. When the geometry of the experiment changed, in particular, when the sharpness of focusing was changed (and hence the position of the waist), the best coincidence between the calculated and experimentally measured dependences was observed for the same values of the weighting energetic coefficients. It should be noted that this technique, analogous to experimental determination of the dependence, is capable of automatic adjustment of the weighting energetic coefficients.

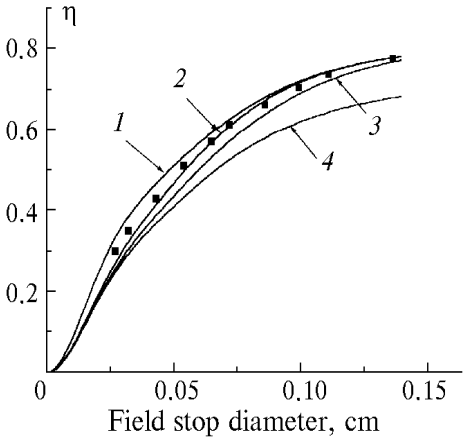

FIG. 4. Dependence of the function η *on the field stop diameter. Here, filled squares show the experimental data and solid lines show the calculated results for different values of the weighting energetic coefficients. Curve 1: the relative contribution from the background component (from the first and second volumes) is* 20%, *the contribution from the third volume is* 25%, *the contribution from the fourth volume is* 25%, *and the contribution from the coherent radiation component (from the fifth and subsequent volumes) is* 30%; *curve 2: the relative contribution from the background component is* 20%, *the contribution from the third volume is* 25%, *the contribution from the fourth volume is* 35%, *and the contribution from the coherent radiation component is* 20%; *curve 3: the relative contribution from the background component is* 20%, *the contribution from the third volume is* 35%, *the contribution from the fourth volume is* 25%, *and the contribution from the coherent radiation component is* 20%; *curve 4: the relative contribution from the background component is* 30%, *the contribution from the third volume is* 25%, *the contribution from the fourth volume is* 25%, *and the contribution from the coherent radiation component is* 30%.

CONCLUSION

It should be noted once again that our theoretical calculations were done for uniform distributions of the refractive index and gain over the cross sections of the medium. These assumptions are not principal. When these phenomena are significant, they can be taken into account in calculations that become more complicated. Moreover, the dependence of the results of calculations from the parameters of the active medium can be used to solve the inverse problem using the given technique, that is, to reconstruct the parameters of the active medium from the changes of the structure of the output radiation. But this problem is beyond the scope of the present paper.

ACKNOWLEDGMENT

The work was supported in part by the Russian Foundation for Basic Researches (Project 96–02–16382–a).

REFERENCES

1. Ya.A. Anan'ev, *Optical Resonators and Laser Radiation Divergence* (Nauka, Moscow, 1979), 328 pp.
2. V.V. Kolosov and V.O. Troitskii, Atmos. Oceanic Opt. **6**, No. 8, 580–583 (1993).
3. A.A. Isaev, M.A. Kazaryan, G.G. Petrash, et al., Kvant. Elektron. **4**, No. 6, 1325–1335 (1977).
4. V.P. Belyaev, V.V. Zubov, A.A. Isaev, et al., Kvant. Elektron. **12**, No. 1, 74–79 (1985).
5. A.A. Zemlyanov and V.V. Kolosov, Atmos. Oceanic Opt. **7**, No. 11–12, 837–840 (1994).
6. V.V. Kolosov, Atmos. Oceanic Opt. **8**, No. 12, 1023–1027 (1995).
7. S.M. Rytov, Yu.A. Kravtsov, and V.I. Tatarskii, *Introduction into Statistical Radiophysics* (Nauka, Moscow, 1978), 464 pp.